A MAJOR PROJECT REPORT

on

Grid connected PV Wind Battery coupled bidirectional DC-DC Luo converter for household applications

Submitted in partial fulfilment for the award of the degree

of

BACHELOR OF TECHNOLOGY

in

ELECTRICAL AND ELECTRONICS ENGINEERING

by

SUMIT DAS (RA1411005010190)

DEVESH TRIPATHI (RA1411005010186)

GAURAV SINGH (RA1411005010172)

Under the guidance of

Mr. B. VINOTHKUMAR

(Assistant Professor (O.G), Department of Electrical and Electronics Engineering)

FACULTY OF ENGINEERING AND TECHNOLOGY

SRM Nagar, Kattankulathur- 603 203
Kancheepuram Dist.

MAY 2018

BONAFIDE CERTIFICATE

Certified that this major project report titled "**Grid connected PV Wind Battery coupled bidirectional DC-DC Luo converter for household Applications**" is the bonafide work of **SUMIT DAS (RA1411005010190) , GAURAV SINGH(RA1411005010172), DEVESH KUMAR (RA1411005010186)** who carried out the project under the supervision of B.VINOTHKUMAR sir. Certified further, that to the best of my knowledge the work reported herein does not form part of any other project report or dissertation on the basis of which a degree or award was conferred on an earlier occasion of this or any other candidate.

Signature of the Guide
Mr. B.VINOTHKUMAR
EEE Department
SRM Institute of science and technology

Signature of the HOD
Dr. K. Vijaya Kumar
EEE Department
SRM Institute of science and technology

Internal Examiner

External Examiner

Date- 28/04/2018

ACKNOWLEDGEMENT

We would like to express my special thanks of gratitude to the managing department of SRM University. Also to the Director (E&T) Dr. C. Muthamizhchelvan. Our sincere thanks to HOD Sir Dr.K.Vijaykumar for providing such good environment in the department for our project analysing.

Our project coordinator Mr.D.SATTINADAN and our project guide Mr.B.VINOTHKUMAR who gave us the opportunity to do this project on the topic "Grid-connected PV-Wind-Battery coupled bidirectional DC-DC Luo converter for household applications", which also helped us in doing a lot of Research. We also came to know about so many new things while making our project and also really thankful to everyone who helped us a lot in finalizing this project.

ABSTRACT

In this Project, a control strategy for power flow management of a grid-connected hybrid photovoltaic (PV)–wind battery- based system coupled bidirectional dc–dc Luo converter is presented. The performance of the proposed control strategy for power flow management under various modes of operation. The effectiveness of the topology and the efficacy of the proposed control strategy are validated proposed system aims to satisfy the load demand, manage the power flow from different sources, inject the surplus power into the grid, and charge the battery from the grid as and when required. Luo converter is used to harness power from wind, while a bidirectional Luo converter is used to harness power from PV along with battery charging/discharging control. A single-phase full-bridge inverter is used for feeding ac loads and interaction with the grid. The proposed converter architecture has reduced number of power conversion stages with less component count and reduced losses compared with existing grid-connected hybrid systems. This improves the efficiency and the reliability of the system. Simulation results obtained using MATLAB/Simulink show the through detailed experimental studies to demonstrate the capability of the system operation in different modes.

TABLE OF CONTENTS

LIST OF FIGURES

FIGURES **PAGE NO.**

CHAPTER 1

INTRODUCTION

1.1 GENERAL

Rapid depletion of fossil fuel reserves, ever increasing energy demand and concerns over climate change motivate power generation from renewable energy sources. Solar photovoltaic (PV) and wind have emerged as popular energy sources due to their eco friendly nature and cost effectiveness. However, these sources are intermittent in nature. Hence, it is a challenge to supply stable and continuous power using these sources. This can be addressed by efficiently integrating with energy storage elements. The interesting complementary behavior of solar insolation and wind velocity pattern coupled with the above-mentioned advantages has led to the research on their integration resulting in the hybrid PV–wind systems. For achieving the integration of multiple renewable sources, the traditional approach involves using dedicated single-input converters one for each source, which are connected to a common dc-bus. However, these converters are not effectively utilized, due to the intermittent nature of the renewable sources. In addition, there are multiple power conversion stages which reduce the efficiency of the system. A significant amount of the literature exists on the integration of solar and wind energy, as a hybrid energy generation system mainly focuses on its sizing and optimization. In the sizing of generators in a hybrid system is investigated. In this system, the sources and storage are interfaced at the dc-link through their dedicated converters. Other contributions are made on their modeling aspects and control techniques for a stand-alone hybrid energy system in. Dynamic performance of a stand-alone hybrid PV–wind system with battery storage is analyzed in. a passivity/sliding mode control is presented which controls the operation of wind energy system to complement the solar energy generating system. Not many attempts are made to optimize the circuit configuration of these systems that could reduce the cost and increase the efficiency and reliability. Integrated converters for PV and wind energy systems are presented. PV–wind hybrid system, has a simple power topology, but it is suitable for stand-alone applications. An integrated four-port topology based on hybrid PV–wind system However, despite simple topology, the control scheme used is complex. To feed the dc loads, a low

capacity multiport converter for a hybrid system is presented. Hybrid PV–wind-based generation of electricity and its interface with the power grid are the important research areas. This system is mainly focused on improving the dc-link voltage regulation. In the six-arm converter topology the outputs of a PV array and wind generators are fed to a luo converter to match the dc-bus voltage. The steady-state performance of a grid-connected hybrid PV and wind system with battery storage is analyzed. This project focuses on system engineering, such as energy production, system reliability, unit sizing, and cost analysis. a hybrid PV–wind system along with a battery is presented, in which both sources are connected to a common dc-bus through individual power luo converters. In addition, the dc-bus is connected to the utility grid through an inverter. The use of multi-input converter for hybrid power systems is attracting increasing attention because of reduced component count, enhanced power density, compactness, and centralized control. Due to these advantages, many topologies are proposed, and they can be classified into three groups, namely, nonisolated, fully isolated, and partially isolated multiport topologies.

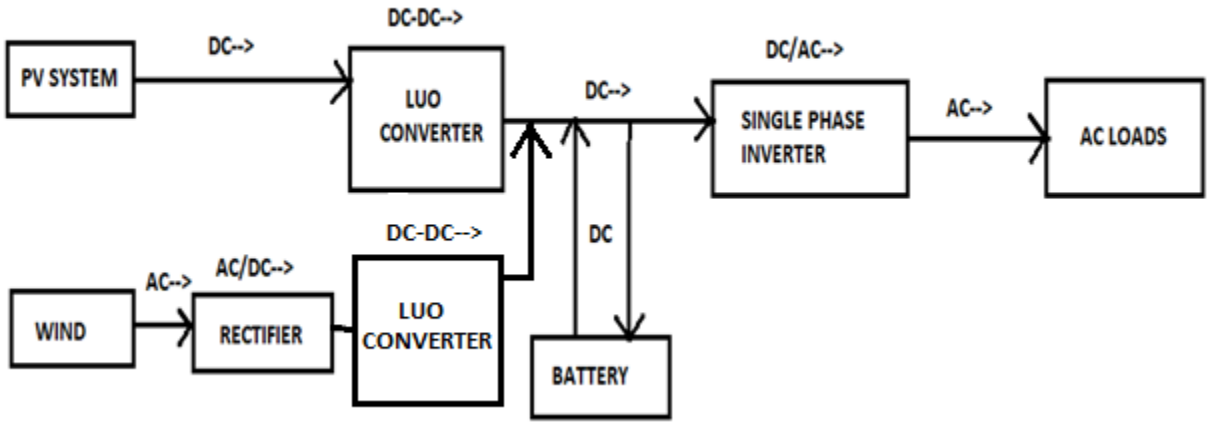

FIGURE 1.1 - BLOCK DIAGRAM

1.2 LITERATURE SURVEY

1.2.1 F. Valenciaga and P. F. Puleston, "Supervisor control for a stand-alone hybrid generation system using wind and photovoltaic energy," *IEEE Trans. Energy Convers.*, vol. 20, no. 2, pp. 398–405, Jun. 2005.

A comprehensive supervisor control for a hybrid system that comprises wind and photovoltaic generation subsystems, a battery bank, and an ac load is developed in this project. The objectives of the supervisor control are, primarily, to satisfy the load power demand and, second, to maintain the state of charge of the battery bank to prevent blackout and to extend the life of the batteries. For these purposes, the supervisor controller determines online the operation mode of both generation subsystems, switching from power regulation to maximum power conversion. Decision criteria for the supervisor based on measurable system variables are presented. Finally, the performance of the supervisor controller is extensively assessed through computer simulation using a comprehensive nonlinear model of the plant.

The rising rate of consumption of nuclear and fossil fuels has drawn worldwide attention to alternative energy technologies. In developed areas, such as the U.S. or the European Union, wind power has been the fastest-growing energy for the last decade, thanks to its increasingly attractive economics, its substantial environmental advantages, and supportive energy policies. However, it is in developing countries where the wind power (in combination with other renewable energies) can play a more substantial role to dramatically improve the quality of life of the people in the immediate future. Particularly, in Latin America, many people live in isolated areas far from the main utility grid. The inability of electrical utilities to meet their needs is a special concern to small rural-based households, schools, and enterprises . It has been proven that small-to-medium-size (10–100 kW) hybrid generation systems based on wind and solar sources may electrify villages, powering lamps and small appliances, small industries, health clinics, and school and community centers.

1.2.2 C. Liu, K. T. Chau, and X. Zhang, "An efficient wind–photovoltaic hybrid generation system using doubly excited permanent-magnet brushless machine," *IEEE Trans. Ind. Electron.*, vol. 57, no. 3, pp. 831–839, Mar. 2010.

With ever-increasing concerns on energy issues, the development of renewable energy sources is becoming more and more attractive. This project first reviews both the wind power and photovoltaic (PV) power generation techniques and their maximum-power-point tracking (MPPT) methods. Then, a new stand-alone wind-PV hybrid generation system is proposed for application to remote and isolated areas. For the wind power generation branch, a new doubly excited permanent-magnet brushless machine is used to capture the maximum wind power by using online flux control. For the PV power generation branch, a single-ended primary inductance converter is adopted to harness the maximum solar power by tuning the duty cycle. The experimental results confirm that the proposed hybrid generation system can provide high efficiency with the use of MPPT.

With their advantages of being abundant in nature and nearly non-pollutant, renewable energy sources have attracted wide attention. Wind power is one of the most promising clean energy sources since it can easily be captured by wind generators with high power capacity. Photovoltaic (PV) power is another promising clean energy source since it is global and can be harnessed without using rotational generators. In fact, wind power and PV power are complementary to some extent since strong winds are mostly to occur during the nighttime and cloudy days whereas sunny days are often calm with weak winds [1]. Hence, a wind–PV hybrid generation system can offer higher reliability to maintain continuous power output than any other individual power generation systems. In those remote or isolated areas, the stand-alone wind–PV hybrid generation system is particularly valuable and attractive.

1.2.3 W. Qi, J. Liu, X. Chen, and P. D. Christofides, "Supervisory predictive control of standalone wind/solar energy generation systems," *IEEE Trans. Control Syst. Technol.*, vol. 19, no. 1, pp. 199–207, Jan. 2011.

This work focuses on the development of a supervisory model predictive control method for the optimal management and operation of hybrid standalone wind-solar energy generation systems. We design the supervisory control system via model predictive control which computes the power references for the wind and solar subsystems at each sampling time while minimizing a suitable cost function. The power references are sent to two local controllers which drive the two subsystems to the requested power references. We discuss how to incorporate practical considerations, for example, how to extend the life time of the equipment by reducing the peak values of inrush or surge currents, into the formulation of the model predictive control optimization problem. We present several simulation case studies that demonstrate the applicability and effectiveness of the proposed supervisory predictive control architecture.

Alternative energy technologies, like wind- and solar based energy generation systems, are receiving national and worldwide attention owing to the rising rate of consumption of nuclear and fossil fuels. In particular, drivers for solar/wind renewable energy systems are the environmental benefits (reduction of carbon emissions due to the use of renewable energy sources and the efficient use of fossil fuels), reduced investment risk, fuel diversification, and energy autonomy, increased energy efficiency (less line losses) as well as potential increase of power quality and reliability and in certain cases, potential grid expansion deferral due to the possibility of generation close to demand. In a recent report of the California Energy Commission, for example, the state's target is to generate from renewable sources the 33% of the energy needed by year 2020, with about 70% of that energy being produced by wind and solar systems ; many other states have similar goals.

1.2.4 F. Giraud and Z. M. Salameh, "Steady-state performance of a grid-connected rooftop hybrid wind-photovoltaic power system with battery storage," *IEEE Trans. Energy Convers.*, vol. 16, no. 1, pp. 1–7, Mar. 2001.

Summary form only given, as follows. This project reports the performance of a 4-kW grid-connected residential wind-photovoltaic system (WPS) with battery storage located In Lowell, MA, USA. The system was originally designed to meet a typical New-England (TNE) load demand with a loss of power supply probability (LPSP) of one day in ten years as recommended by the utility company. The data used in the calculation was wind speed and irradiance of Logan Airport Boston (LAB) obtained from the National Climate Center In North Carolina. The present performance study is based on two-year operation (May 96-Apr 98) of the WPS. Unlike conventional generation, the wind and the sunrays are available at no cost and generate electricity pollution-free. Around noontime, the WPS satisfies its load and provides additional energy to the storage or to the grid. On-site energy production is undoubtedly accompanied with minimization of environmental pollution, reduction of losses in power systems transmission and distribution equipment, and supports the utility in demand side management (DSM). This project includes discussion on system reliability, power quality, loss of supply, and effects of the randomness of the wind and the solar radiation on system design.

1.2.5 S.-K. Kim, J.-H. Jeon, C.-H. Cho, J.-B. Ahn, and S.-H. Kwon, "Dynamic modeling and control of a grid-connected hybrid generation system with versatile power transfer," *IEEE Trans. Ind. Electron.*, vol. 55, no. 4, pp. 1677–1688, Apr. 2008.

This project presents power-control strategies of a grid-connected hybrid generation system with versatile power transfer. The hybrid system is the combination of photovoltaic (PV) array, wind turbine, and battery storage via a common dc bus. Versatile power transfer was defined as multi-modes of operation, including normal operation without use of battery, power dispatching, and power averaging, which enables grid- or user-friendly operation. A supervisory control regulates power generation of the individual components so as to enable the hybrid system to operate in the proposed modes of operation. The concept and principle of the hybrid system and its control were described. A simple technique using a low-pass filter was introduced for power averaging. A modified hysteresis-control strategy was applied in the battery converter. Modeling and simulations were based on an electromagnetic-transient-analysis program. A 30-kW hybrid inverter and its control system were developed. The simulation and experimental results were presented to evaluate the dynamic performance of the hybrid system under the proposed modes of operation.

The integration of renewable energy sources and energy-storage systems has been one of the new trends in power-electronic technology. The increasing number of renewable energy sources and distributed generators requires new strategies for their operations in order to maintain or improve the power-supply stability and quality. Combining multiple renewable resources via a common dc bus of a power converter has been prevalent because of convenience in integrated monitoring and control and consistency in the structure of controllers as compared with a common ac type. There are some previous works on similar hybrid systems. Dynamic performance of a stand-alone wind and solar system with battery storage was analyzed. A wind turbine-system model was developed and compared with a real system. Several methodologies for optimal design or unit sizing of stand-alone or grid-connected hybrid systems have been proposed using steady-state analysis.

CHAPTER 2

EXISTING SYSTEM AND PROPOSED SYSTEM

Hybrid PV–wind-based generation of electricity and its interface with the power grid are the important research areas. A multi-input hybrid PV–wind power generation system which has a luo dc–dc converter and a full-bridge single phase inverter. This system is mainly focused on improving the dc-link voltage regulation. In the six-arm converter topology proposed, the outputs of a PV array and wind generators are fed to a boost converter to match the dc-bus voltage. The steady-state performance of a grid-connected hybrid PV and wind system with battery storage is analyzed. This project focuses on system engineering, such as energy production, system reliability, unit sizing, and cost analysis. In a hybrid PV–wind system along with a battery is presented, in which both sources are connected to a common dc-bus through individual power luo converters. In addition, the dc-bus is connected to the utility grid through an inverter. The use of multi-input converter for hybrid power systems is attracting increasing attention because of reduced component count, enhanced power density, compactness, and centralized control. Due to these advantages, many topologies are proposed, and they can be classified into three groups, namely, non-isolated, fully isolated, and partially isolated multiport topologies.

A grid-connected hybrid PV–wind-battery-based power evacuation scheme for household application is proposed. The proposed hybrid system provides an elegant integration of PV and wind source to extract maximum energy from the two sources. A versatile control strategy which achieves a better utilization of PV, wind power, battery capacities without effecting life of battery, and power flow management in a grid-connected hybrid PV–wind-battery-based system feeding ac loads is presented. Detailed simulation studies are carried out to ascertain the viability of the scheme. The experimental results obtained are in close agreement with simulations and are supportive in demonstrating the capability of the system to operate either in grid feeding or in stand-alone modes. The proposed configuration is capable of supplying uninterruptible power to ac loads, and ensures the evacuation of surplus PV and wind power into the grid.

CHAPTER 3

CIRCUIT DIAGRAM

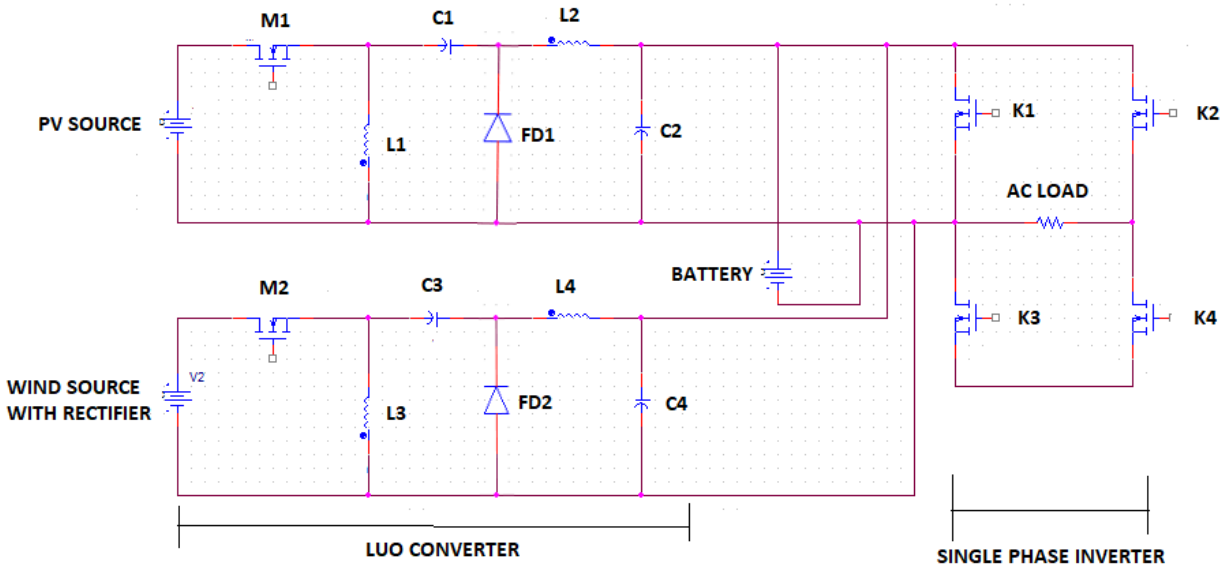

FIGURE 3.1 CIRCUIT DIAGRAM

The circuit diagram consist of a PV source , wind source and a battery as a power bank. There are two luo converters for PV as well as wind separately. Mosfets are used as a triggering switch. Inductors and capacitors are used for charging and discharging purpose. To convert dc to ac single phase full bridge inverter is used to supply power to the ac load. The input of photovoltaic cell is sun light and the output current and voltage is 1A and 69.9V. The input of wind is mechanical energy which is converted into electrical energy. The output voltage of wind energy is around 145V and converter output is 390V. Asynchronous generator is used to convert mechanical energy into electrical energy. The load which we are using is resistive load.

CHAPTER 4

COMPONENTS DETAILS

4.1 PV MODEL

Photovoltaic (PV) cells are made of, semiconducting materials that can convert incident radiation in the solar spectrum to electric currents. PV cells are most commonly made of silicon, and come in two varieties, crystalline and thin-film type. When a photon is absorbed by a semiconducting material, it increases the energy of a valence band electron, thrusting it into the conduction band. This occurs when the energy of incident photons is higher than the bandgap energy. The conducting band electron then produces a current that moves through the semiconducting material.

A single solar cell cannot provide required useful output. So, to increase output power level of a PV system, it is required to connect number of such PV solar cells. A solar module is normally series connected sufficient number of solar cells to provide required standard output voltage and power. One solar module can be rated from 3 watts to 300 watts. The solar modules or PV modules are commercially available basic building block of a solar electric power generation systems.

Actually a single solar PV cell generates very tiny amount that is around 0.1 watt to 2 watts. But it is not practical to use such low power unit as building block of a system. So required number of such cells are combined together to form a practical commercially available solar unit which is known as solar module or PV module.

In a solar module the solar cells are connected in same fashion as the battery cell units in a battery bank system. That means positive terminals of one cell connected to negative terminal voltage of solar module is simple sum of the voltage of individual cells connected in series in the module.

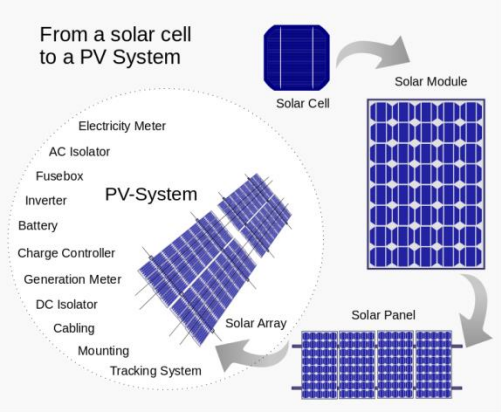

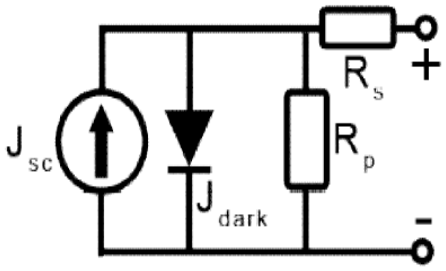

Fig. 2. Equivalent circuit of PV model.

FIGURE 4.1.1 SOLAR MODULE

FIGURE 4.1.2 EQUIVALENT CIRCUIT

The PV cell output voltage is a function of the photocurrent that mainly determined by load current depending on the solar irradiation level during the operation (1)

$$V_c = \frac{Ak\,T_c}{e} \ln\left(\frac{I_{ph} + I_o - I_c}{I_o}\right) - R_s I_c \quad \text{----- (1)}$$

Where the symbols are defined as follows:

e: electron charge (1.602 × 10-19 C).

k: Boltzmann constant (1.38 × 10-23 J/oK).

Ic: cell output current, A. Iph: photocurrent, function of irradiation level and junction temperature (5 A).

I0: reverse saturation current of diode (0.0002 A).

Rs: series resistance of cell (0.001 Ω).

Tc: reference cell operating temperature (20 °C).

Vc: cell output voltage, V.

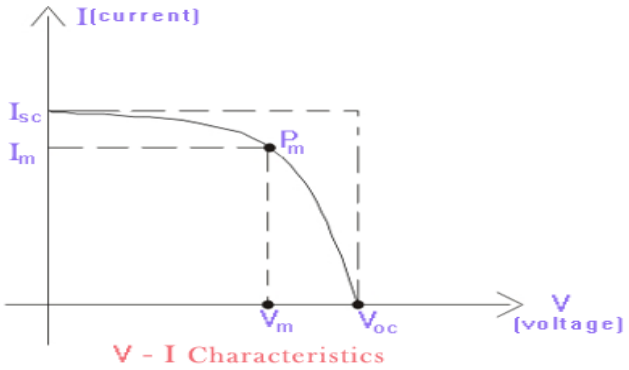

FIGURE 4.1.3 V-I CHARACTERISTICS

Both k and Tc should have the same temperature unit, either Kelvin or Celsius.

V-I Characteristic of Solar Module

If we draw a graph by taking X-axis as voltage axis and Y-axis as currents of a solar module, then the graph will represent V-I characteristic of a solar module.

4.2 WIND MODEL

Wind turbines convert mechanical energy produced by the wind to electrical energy. To use this electrical energy, voltage and frequency regulation are needed. A wind turbine generator system (WTGS) transforms the energy present in the blowing wind into electrical energy. Wind energy is transformed into mechanical energy by a wind turbine that has several blades. It usually includes a gearbox that matches the turbine low speed to the higher speed of the generator.

FIGURE 4.2.1 WIND MODEL

The model of a wind turbine is developed on the basis of the steady-state power characteristics of the turbine. The mechanical power produced by a wind turbine is shown in Equation (2).

$$P_m = \frac{1}{2} C_p(\lambda, \beta) \rho A v^3 \quad \text{-------- (2)}$$

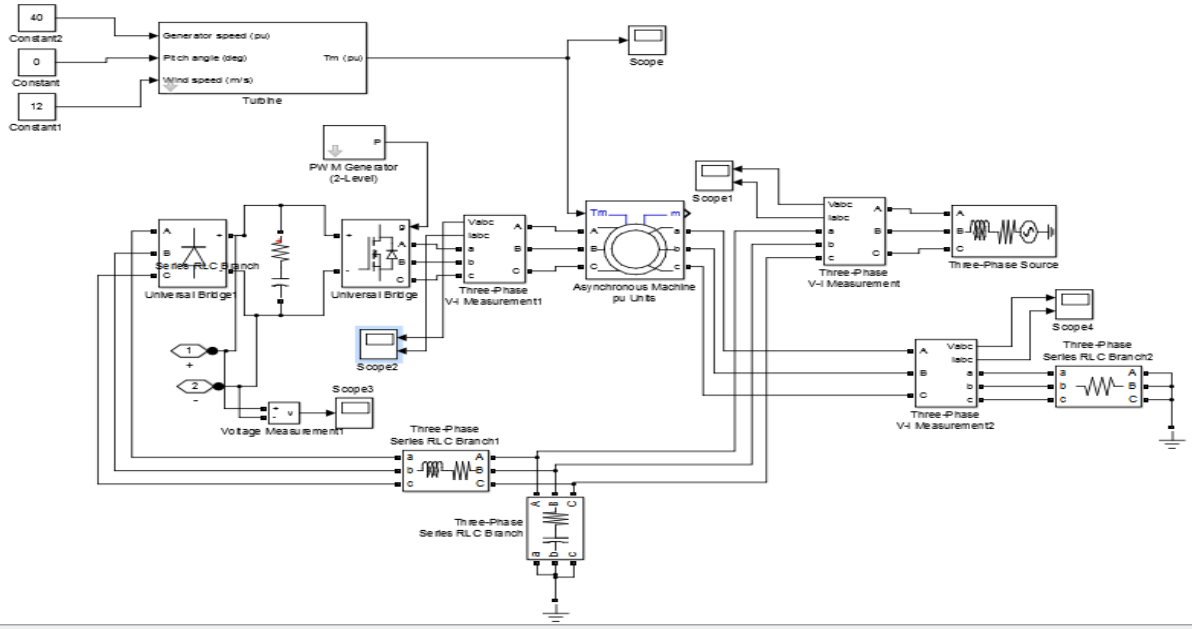

FIGURE 4.2.2 SIMULATION OF A WIND MODEL

The Simulink model of the studied wind turbine is shown in Figure 3. In Eq. (1), Pm is the mechanical output power of the turbine (W), Cp is the performance coefficient of the turbine, λ is the tip speed ratio of the rotor blade tip speed to the wind speed (in degrees), β is the blade pitch angle (in degrees), ρ is the air density (kg/m3), A is the turbine swept area (m2), and v is the wind speed (m/s). The expression "Cp (λ, β)" is calculated by using Eqs. (3) and (4).

$$C_P(\lambda,\beta) = C_1\left(\frac{C_2}{\lambda_1} - C_3\beta - C_4\right)e^{\frac{C_5}{\lambda_4}} + C_6\lambda \quad \text{---- (3)}$$

$$\frac{1}{\lambda_1} = \frac{1}{\lambda + 0.08\,\beta} - \frac{0.035}{\beta^3 + 1} \quad \text{----- (4)}$$

Coefficients C1 through C6 are: C1 =0.5176, C2 =116, C3 =0.4, C4 =5,

C5 =21, and C6 =0.0068. β is equal to 0, but, if necessary, this value can be changed.

4.3 DOUBLY FED INDUCTION GENERATOR ELECTRICAL MODEL:

The basic configuration of a DFIM is sketched . The most significant feature of this kind of wound-rotor machine is that it has to be fed from both stator and rotor side. Normally, the stator is directly connected to the grid and the rotor is interfaced through a variable frequency power converter. In order to cover a wide operation range from sub-synchronous to super-synchronous speeds, the power converter placed on the rotor side has to be able to operate with power flowing in both directions. This is achieved by means of a back-to-back PWM inverter configuration. The operating principle of a DFIM can be analyzed using the classic theory of rotating fields and the well-known d-q model, as well as both three-to-two and two-to three axes transformations.

4.4 BATTERY MODEL

The mathematical modeling of Li-Ion battery is used in the simulation. The open voltage source is calculated with a non- linear equation based on the actual SOC of the battery as follows

$$V_{batt} = E_{batt} - R_i \quad \text{------ (5)}$$

During discharge:

$$E_{batt} = E_e - K\frac{Q}{Q-it}it - k\frac{Q}{Q-it}i^* + A\exp(-Bit) \quad \text{----- (6)}$$

During charge:

$$E_{batt} = E_e - K\frac{Q}{Q-it}it - k\frac{Q}{it+0.1Q}i^* + A\exp(-Bit) \quad \text{-- (7)}$$

Where, E_{batt} is the no-load voltage,

Eo is the battery constant voltage,

K is the polarization constant,

Q is the battery capacity, it is the actual battery charge,

i* is the low frequency current dynamics,

A is the exponential zone amplitude,

B is the exponential zone time constant inverse (Ah)-1,

V_{batt} is the battery voltage, and i is the battery current.

The main feature of this battery model is that the parameters can easily be deduced from a manufacturer's discharge curve.

4.5 RECTIFIER CIRCUIT-

230V AC power is converted into 12V AC (12V RMS value wherein the peak value is around 17V), but the required power is 5V DC; for this purpose, 17V AC power must be primarily converted into DC power then it can be stepped down to the 5V DC.

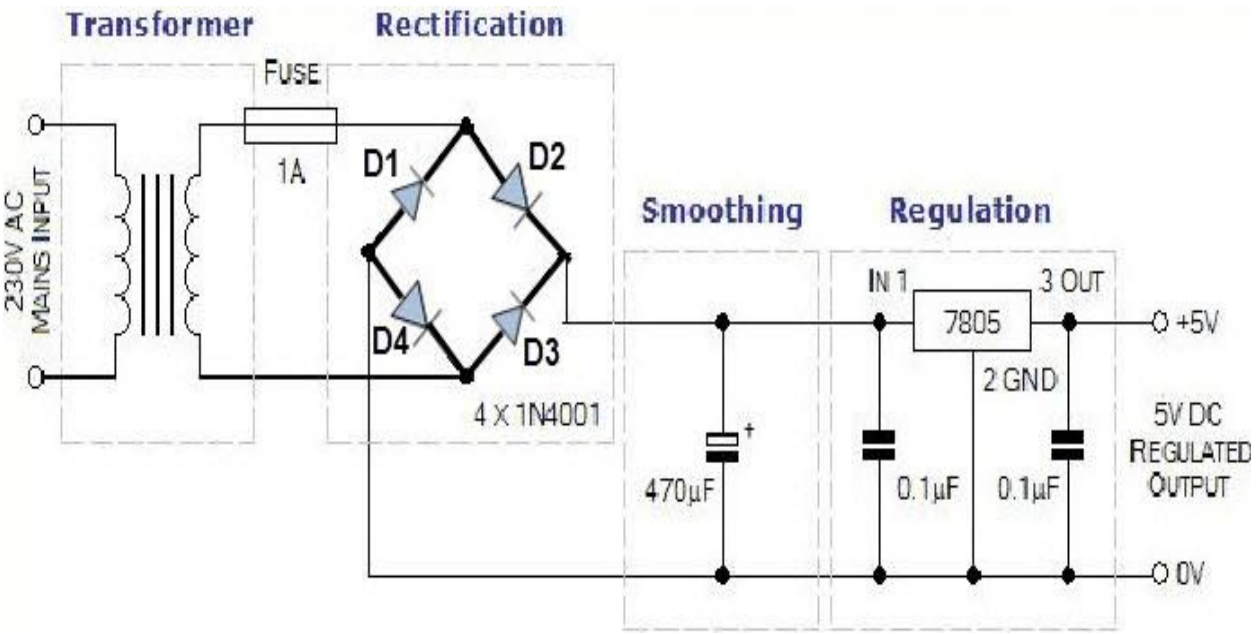

FIGURE 4.5.1 BRIDGE RECTIFIER

But first and foremost, we must know how to convert AC to DC? AC power can be converted into DC using one of the power electronic converters called as Rectifier. There are different types of rectifiers, such as half-wave rectifier, full-wave rectifier and bridge rectifier. Due to the advantages of the bridge rectifier over the half and full wave rectifier, the bridge rectifier is frequently used for converting AC to DC.Bridge rectifier consists of four diodes which are connected in the form a bridge. We know that the diode is an uncontrolled rectifier which will conduct only forward bias and will not conduct during the reverse bias. If the diode anode voltage is greater than the cathode voltage then the diode is said to be in forward bias. During positive half cycle, diodes D2 and D4 will conduct and during negative half cycle diodes D1 and D3 will conduct. Thus, AC is converted into DC; here the obtained is not a pure DC as it consists of pulses. Hence, it is called as pulsating DC power.

4.6 SMOOTHING THE RIPPLE USING FILTER

15V DC can be regulated into 5V DC using a step-down converter, but before this, it is required to obtain pure DC power. The output of the diode bridge is a DC consisting of ripples also called as pulsating DC. This pulsating DC can be filtered using an inductor filter or a capacitor filter or a resistor-capacitor-coupled filter for removing the ripples. Consider a capacitor filter which is frequently used in most cases for smoothing.

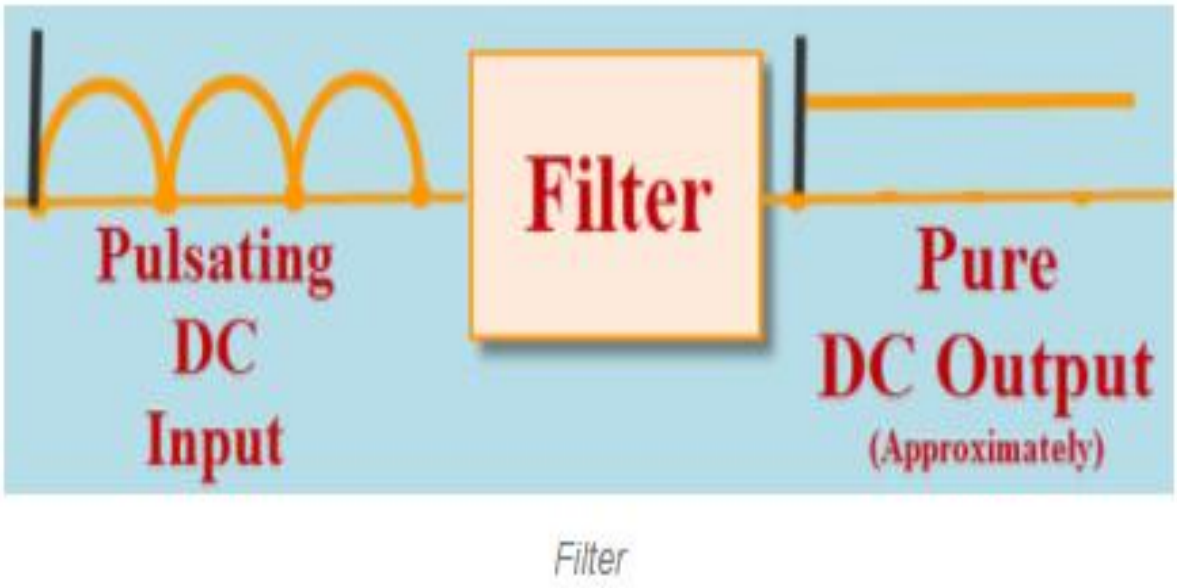

FIGURE 4.6.1 FILTER

We know that a capacitor is an energy storing element. In the circuit, capacitor stores energy while the input increases from zero to a peak value and, while the supply voltage decreases from peak value to zero, capacitor starts discharging. This charging and discharging of the capacitor will make the pulsating DC into pure DC.

4.7 VOLTAGE REGULATOR

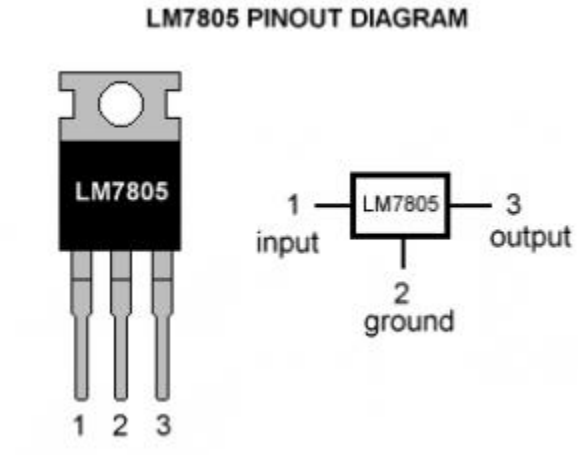

FIGURE 4.7.1 VOLTAGE REGULATOR

15V DC voltage can be stepped down to 5V DC voltage using a DC step-down converter called as voltage regulatorIC7805. The first two digits '78' of IC7805 voltage regulator represent positive series voltage regulators and the last two digits '05' represents the output voltage of the voltage regulator.

4.8 DSPIC MICROCONTROLLER

The dsPIC30F devices contain extensive Digital Signal Processor (DSP) functionality within a high-performance 16-bit microcontroller (MCU) architecture.

FIGURE 4.8.1 dsPIC30F2010

4.8.1 High-Performance Modified RISC CPU:

• C compiler optimized instruction set architecture

• 84 base instructions with flexible addressing modes

• 24-bit wide instructions, 16-bit wide data path

• 12 Kbytes on-chip Flash program space

• 512 bytes on-chip data RAM

• 1 Kbyte non-volatile data EEPROM

• 16 x 16-bit working register array

• Up to 30 MIPs operation: - DC to 40 MHz external clock input

• 27 interrupt sources

• Three external interrupt sources

• 8 user selectable priority levels for each interrupt

• 4 processor exceptions and software traps

4.8.2 DSP Engine Features:

• Modulo and Bit-Reversed modes

• Two, 40-bit wide accumulators with optional saturation logic

• 17-bit x 17-bit single cycle hardware fractional/ integer multiplier

• Single cycle Multiply-Accumulate (MAC) operation

• 40-stage Barrel Shifter

• Dual data fetch

4.8.3 Peripheral Features:

• High current sink/source I/O pins: 25 mA/25 mA

• Three 16-bit timers/counters; optionally pair up 16-bit timers into 32-bit timer modules

• Four 16-bit Capture input functions

• Two 16-bit Compare/PWM output functions - Dual Compare mode available

• 3-wire SPITM modules (supports 4 Frame modes)

• I2CTM module supports Multi-Master/Slave mode and 7-bit/10-bit addressing

• Addressable UART modules with FIFO buffers

.8.4 Motor Control PWM Module Features:

• 6 PWM output channels - Complementary or Independent Output modes - Edge and Center Aligned modes

• 4 duty cycle generators

• Dedicated time base with 4 modes

• Programmable output polarity

• Dead time control for Complementary mode

• Manual output control

• Trigger for synchronized A/D conversions

4.8.5 PIN DIAGRAM OF dsPIC30F2010

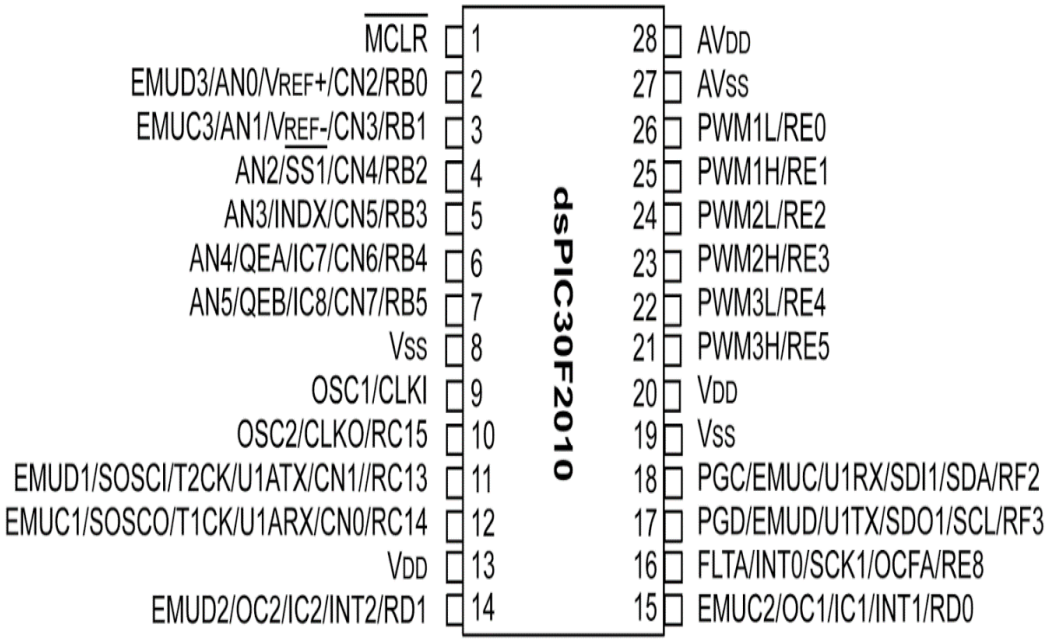

FIGURE 4.8.2 PIN DIAGRAM dsPIC30F2010

This controller contains 28 pins in that six pins are PWM pins. Mainly controllers used in this project to generate gating pulses for switches. Pulse Width Modulation (PWM) is a technique in which the width of a pulse is modulated keeping the time period of the wave constant. The ON time and OFF time can have any different values in the wave cycles, but the sum of the ON time and OFF time remains same for the entire cycles. With the help of the modulation of the width of a pulse in a period of the wave, they can generate any required voltage with the help of a proper filter circuits. The filter circuits are used for generating the voltage corresponding to a modulated wave. This feature of the PWM wave is making use in so many digital systems like DC motor control, audio devices, simple decoration light controls etc. The PIC30F2010 has an inbuilt PWM module which can generate continuous PWM waves.

4.9 DRIVER CIRCUIT

4.9.1 OPTO COUPLER

Opto-isolators or Opto-couplers, are made up of a light emitting device, and a light sensitive device, all wrapped up in one package, but with no electrical connection between the two, just a beam of light. The light emitter is nearly always an LED. The light sensitive device may be a photodiode, phototransistor, or more esoteric devices such as thyristors, TRIACs etc.

MOSFET driver TL250 like other MOSFET drivers have input stage and output stage. It also have power supply configuration. TLP250 is more suitable for MOSFET and IGBT. The main difference between TLP250 and other MOSFET drivers is that TLP250 MOSFET driver is optically isolated. Its mean input and output of TLP250 MOSFET driver is isolated from each other. Its works like a optocoupler. Input stage have a light emitting diode and output stage have photo diode. Whenever input stage LED light falls on output stage photo detector diode, output becomes high.

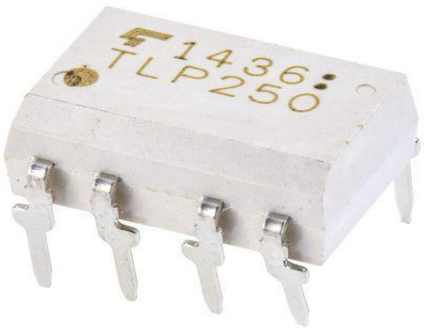

FIGURE 4.9.1 PIN CONFIGURATION OF TLP250

- Pin layout of TLP250 is given below. It is clearly shown in figure that led at input stage and photo detector diode at output stage is used to provide isolation between input and output. Pin number 1 and 4 are not connected to any point. Hence, they are not in use. Pin 2 is anode point of input stage light emitting diode and pin 3 is cathode point of input stage. Input is provided to pin number 2 and 3. Pin number 8 is for supply connection. Pin number

5 is for ground of power supply.Pin number one and four is not connected to any point physically. Therefore, they are not in use.

- Pin number 8 is use to provide power supply to TLP250 and pin number 5 is ground pin which provides return path to power supply ground. Maximum power supply voltage between 15-30 Volt dc can be given to TLP250. But it also depends on temperature of environment in which you are using TLP250.

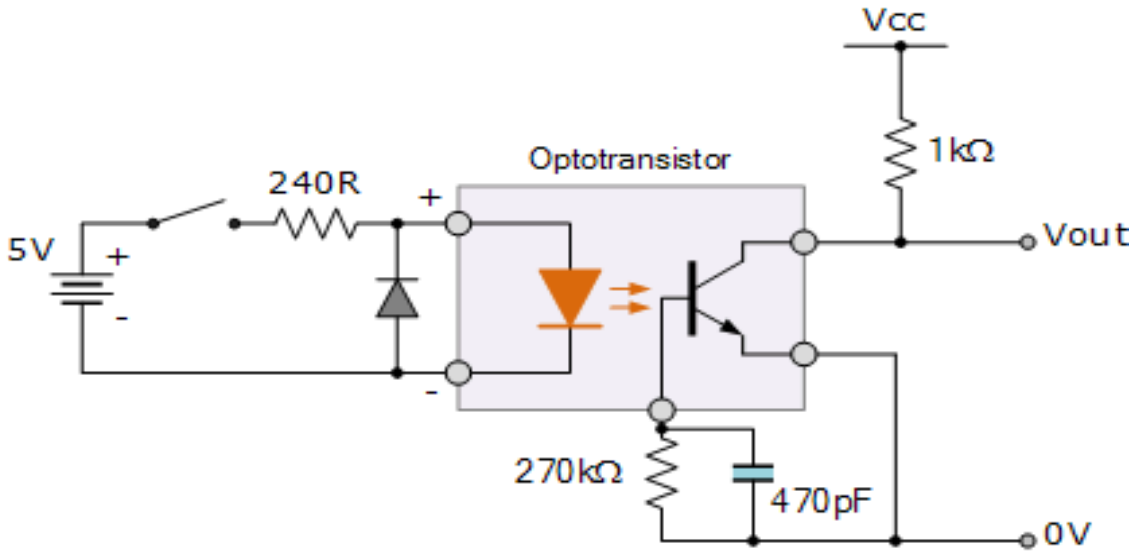

FIGURE 4.9.2 CIRCUIT DIAGRAM OF TLP250 DRIVER CIRCUIT

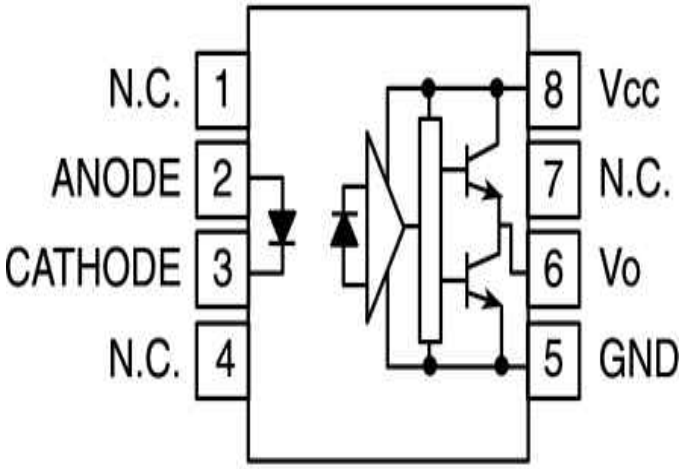

FIGURE 4.9.3 PIN DIAGRAM OF TLP250

- Pin number 2 and 3 are anode and cathode points of input stage LED. It works like a normal light emitting diode. It has similar characteristics of forward voltage and input current. Maximum input current is in the range of 7-10mA and forward voltage drop is about 0.8 volt. TLP250 provides output from low to high with minimum threshold current of 1.2mA and above.

- Pin number six and seven is internally connected to each other. Output can be taken from either pin number 6 and 7. Totem pole configuration of two transistor is used in TLP250. In case of high input, output becomes high with output voltage equal to supply voltage and in case of low input, output become low with output voltage level equal to ground.

Assume a photo-transistor device as shown. Current from the source signal passes through the input LED which emits an infra-red light whose intensity is proportional to the electrical signal.This emitted light falls upon the base of the photo-transistor, causing it to switch-ON and conduct in a similar way to a normal bipolar transistor.The base connection of the photo-transistor can be left open (unconnected) for maximum sensitivity to the LEDs infrared light energy or connected to ground via a suitable external high value resistor to control the switching sensitivity making it more stable and resistant to false triggering by external electrical noise or voltage transients.

When the current flowing through the LED is interrupted, the infrared emitted light is cut-off, causing the photo-transistor to cease conducting. The photo-transistor can be used to switch current in the output circuit. The spectral response of the LED and the photo-sensitive device are closely matched being separated by a transparent medium such as glass, plastic or air. Since there is no direct electrical connection between the input and output of an optocoupler, electrical isolation up to 10kV is achieved.

CHAPTER 5

FUNCTIONS OF LUO CONVERTER

5.1 MODES OF OPERATION

5.1.1 MODE-1

- When the switch is ON.
- The inductor L1 is charged by the supply voltage E.
- At the same time, the inductor L2 absorbs the energy from source and the capacitor C1.
- The load is supplied by the capacitor C2.

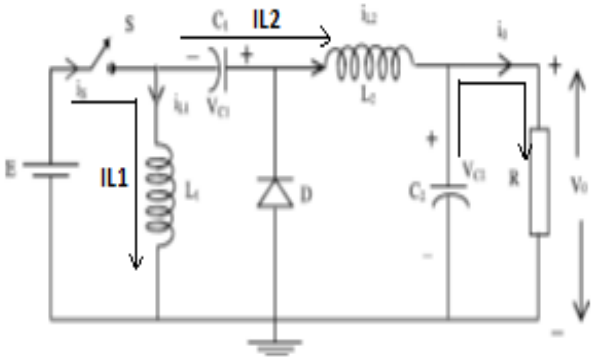

FIGURE 5.1.1.1 LUO CONVERTER CIRCUIT WITH SWITCH ON

5.1.2 MODE-2

- When switch is in OFF state.
- the current is drawn from the source becomes zero.
- Current IL1 flows through the freewheeling diode to charge the capacitor C1.
- Current IL2 flows through C2 –R circuit and the freewheeling diode FD.

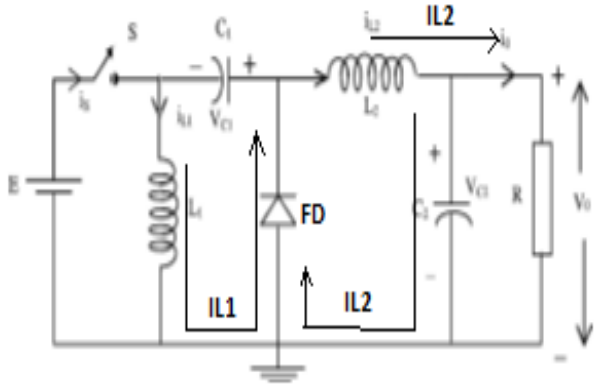

FIGURE 5.1.2.1 LUO CONVERTER CIRCUIT WITH SWITCH OFF

5.2 MODELLING OF ELEMENTARY LUO CONVERTER

5.2.1 USING STATE SPACE METHOD

Apply KVL Determine A, B, C, E Matrices Figure 1 shows elementary Luo converter. In this positive output Luo converter, there are two states i.e., when switch is on and when switch is off. During each state we write the following Equation 1 and 2:

$$x^{'} = A_1 x + B_1 V_d \quad during\, dT_s$$

$$x^{'} = A_2 x + B_2 V_d \qquad \text{during}(1-d)T_s$$

where, A1+ A2 are state matrices and B1 and B2 are vectors. Let x1 be inductor current, x2 represent voltage across capacitor 1, x3 represent voltage across capacitor 2. Figure 2 and 3 shows the turn on and turn off condition of luo converter.

For turn on:

$$\begin{pmatrix} x_1^1 \\ x_2^1 \\ x_3 \end{pmatrix} = \begin{pmatrix} 0 & \frac{1}{L} & 0 \\ \frac{-1}{C_1} & \frac{-1}{(R_1 C_{1)}} & 0 \\ 0 & 0 & \frac{-1}{RC_2} \end{pmatrix} \begin{pmatrix} x_1 \\ x_2 \\ x_3 \end{pmatrix} + \begin{pmatrix} 0 \\ \frac{1}{(R_1 C_1} \\ 0 \end{pmatrix} V_d$$

For turn off:

$$\begin{pmatrix} x_1^1 \\ x_2^1 \\ x_3^1 \end{pmatrix} = \begin{pmatrix} 0 & \frac{1}{L} & \frac{-1}{L} \\ \frac{-1}{C_1} & 0 & 0 \\ \frac{-1}{C_2} & 0 & \frac{-1}{RC_2} \end{pmatrix} \begin{pmatrix} x_1 \\ x_2 \\ x_3 \end{pmatrix} + \begin{pmatrix} \frac{1}{L} \\ 0 \\ 0 \end{pmatrix} V_d$$

$$A=\begin{pmatrix} 0 & \frac{1}{L} & \frac{-(1-D)}{L} \\ \frac{-1}{C_1} & \frac{-D}{(R_1C_0} & 0 \\ \frac{(1-D)}{C_2} & 0 & \frac{-1}{RC_2} \end{pmatrix} B=\begin{bmatrix} \frac{(1-D)}{L} \\ \frac{D}{R_1C_1} \\ 0 \end{bmatrix} C=(0\,0\,1)$$

Using Laplace transformation:

$$S\hat{x}(s)=A\hat{x}(s)+\left[(A_1-A_2)\times+(B_1-B_2)V\right]\hat{d}(s)$$
$$\hat{x}(s)=\left[SI-A\right]^{-1}\left[(A_1-A_2)\times+(B_1-B_2)V\right]\hat{d}(s)$$

$$\frac{\hat{v}_0(s)}{\hat{d}(s)}=C\left[SI-A\right]^{-1}\left[(A_1-A_2)\times+(B_1-B_2)V_d\right]+(C_1-C_2)X$$

Circuit Averaging Technique

In ON condition:

$$V_L(t)=V_g(t)$$
$$iC_1(t)=i_g(t)-i(t)$$
$$iC_2(t)=\frac{-V_0}{R}$$

OFF condition:

$$V_L(t)=2V_g(t)-V_0(t)$$
$$iC_1(t)=i_g(t)$$
$$iC_2(t)=i_g(t)-\frac{V_0}{R}$$
$$V_L(t)=DV_g(t)+D^1(2V_g(t)-V_0(t))$$

$$iC_1(t)=D(i_g(t)\pm i(t))+D^1(i_g(t))$$

$$i_{C2}(t)=D\left(\frac{-V_0}{R}\right)+D^1(i_g(t)-\frac{V_0}{R}$$

$$\frac{\hat{v}_0(s)}{\hat{d}(s)}=V_g\left[\frac{-SL\left(\frac{2-D}{(1-D)^2}\right)+R}{S^2LRC_2+SL+R(1-D)^2}\right]$$

The transfer functions obtained in the state space averaging and circuit averaging technique are the same and it is shown in the Equation 3 and 8.

CHAPTER 6
HARDWARE OUTPUT

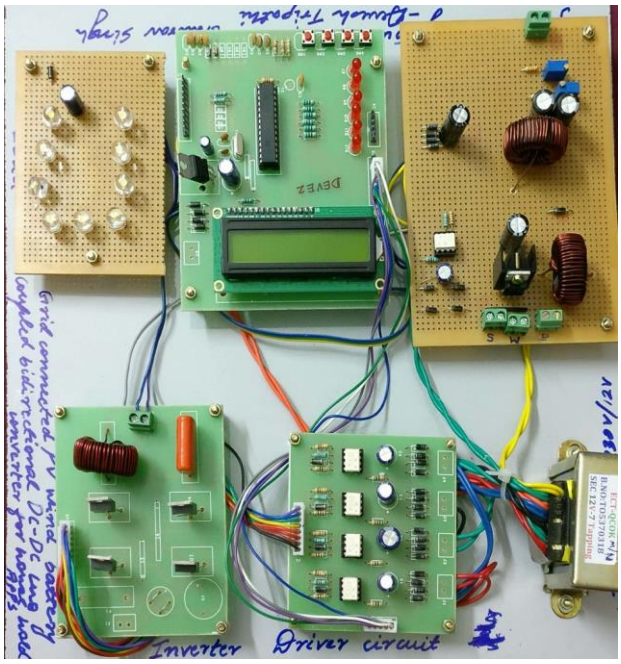

FIGURE 6.1 HARDWARE MODEL

HARDWARE DETAILS	
COMPONENTS	**RATING AND USAGE**
PV PANEL	12V 5W DC
WIND MODULE	12V AC
TLP250	DRIVER IC
dsPIC30F2010	CONTROLLER
DIODE	IN4007
CAPACITOR	470MF
LED(LOAD)	3.3V-4
INDUCTOR	100MH
VOLTAGE REGULATOR	7805

FIGURE 6.2 HARDWARE RATINGS

6.1 WORKING

In the project, when the switch is on then the transformer convert 230V ac supply to 12V ac supply which on further convert into 12V dc using full wave bridge rectifier. The 12V dc supply passes through the voltage regulator 7805 to convert into 5V dc which is the threshold voltage to run the dsPIC microprocessor. The dsPIC30F2010 is a controller microprocessor which provide 5V square wave pulse to the driver circuit TLP250. The optocoupler driver circuit converts the 5V pulse to 12V pulse so as to satisfy the mosfet pulse. There are 5 mosfet used, 4 on single phase inverter and 1 on luo converter.

For the further output the transformer provides 12V supply to the luo converter which boost the dc voltage upto 40V and current 1.43V with a power rating of 57W. Due to the lack of funding in the project the wind source is not shown according to our proposed system.

RESULTS

7.1 SIMULATION

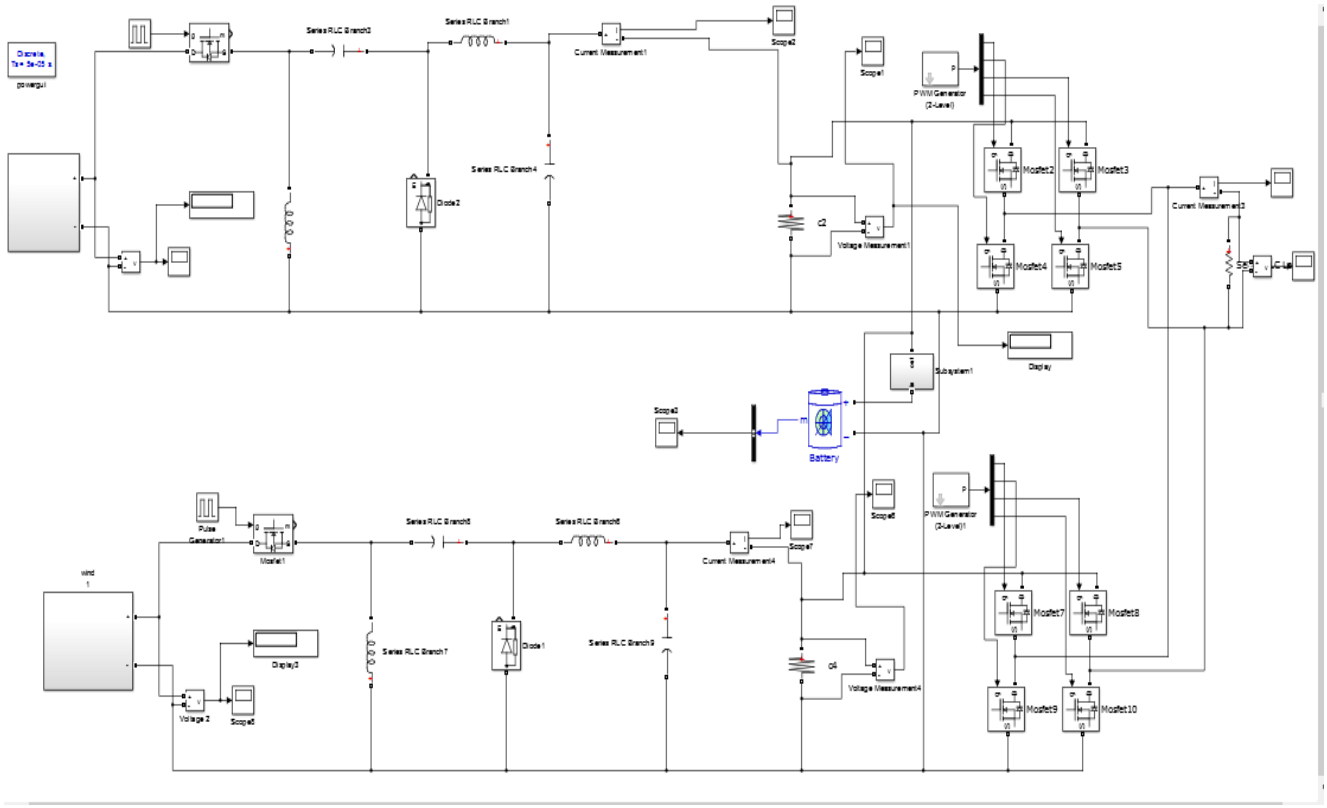

FIGURE 7.1.1 MATLAB Simulink of the Grid-Connected PV-Wind-Battery-Bidirectional DC-DC Luo Converter for Household Applications

In this simulation,the modelling of solar and wind system is accomplished. the photovoltaic powe rating is 70W. The output of solar is 70V and 1A. The simulation consist of a luo converter which is a proposed system of our project. To convert the DC voltage to AC single phase bridge rectifier is used.

7.2 OUTPUT WAVEFORMS

The overall output waveforms of the project is shown here. The output voltage is 388V and the output current is 3.8A. Overall power rating is 1474W. To satisfy the load demand step down transformer is used. The luo converter output is shown . It harness upto 388V and it also charges the battery as well it supplies power to loads.

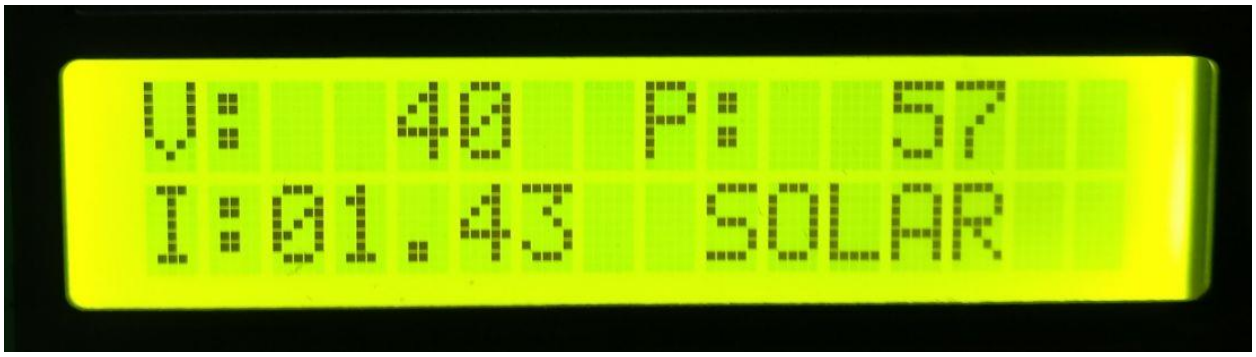

FIGURE 7.2.1 HARDWARE OUTPUT OF SOLAR

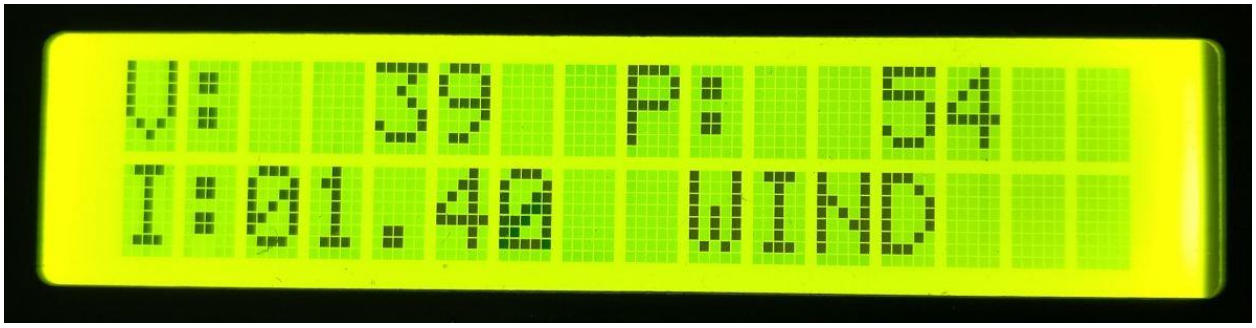

FIGURE 7.2.2 HARDWARE OUTPUT OF WIND

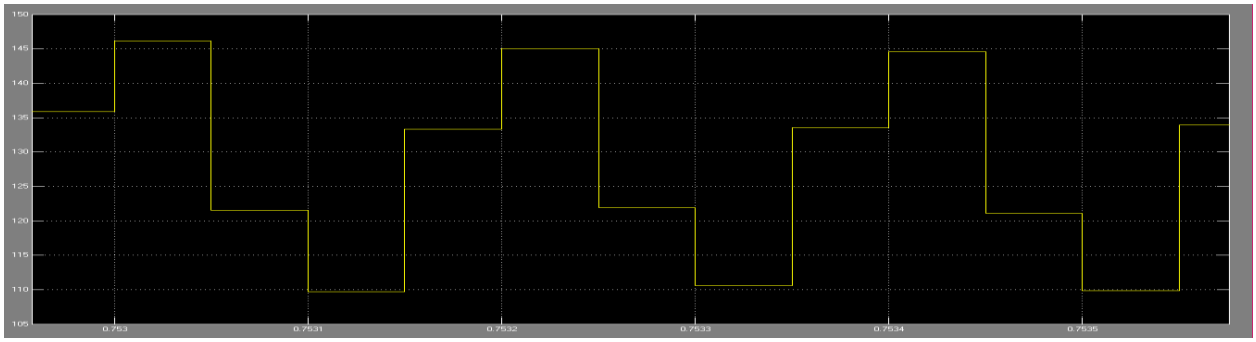

FIGURE 7.2.4 OUTPUT OF WIND MODELLING

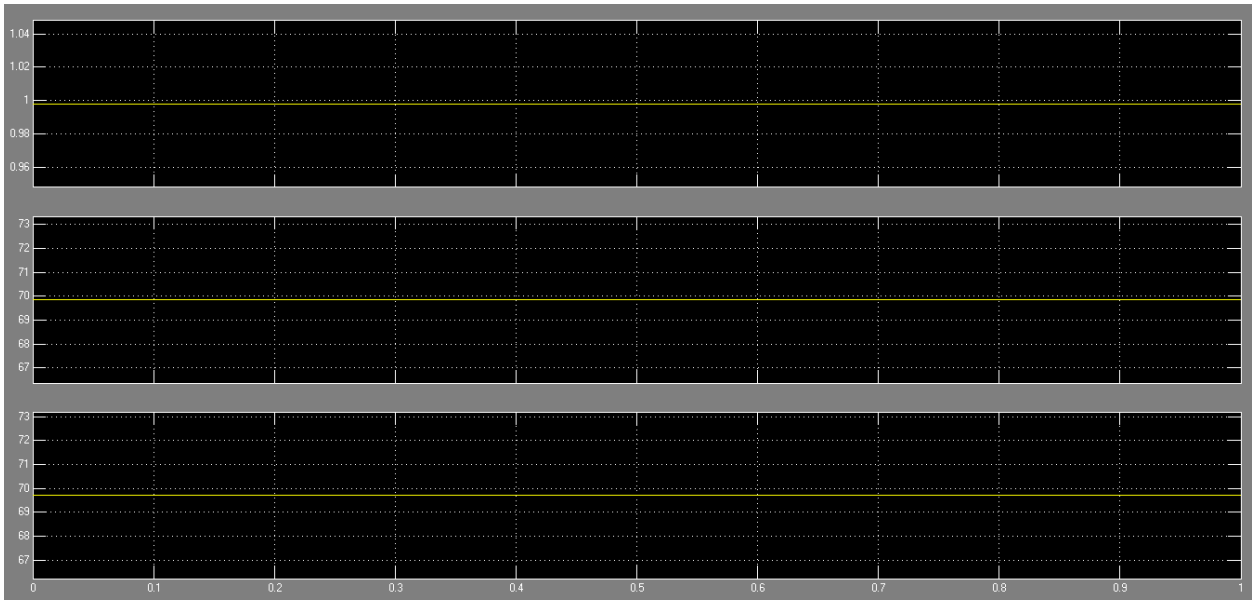

FIGURE 7.2.3 OUTPUT OF SOLAR PANEL

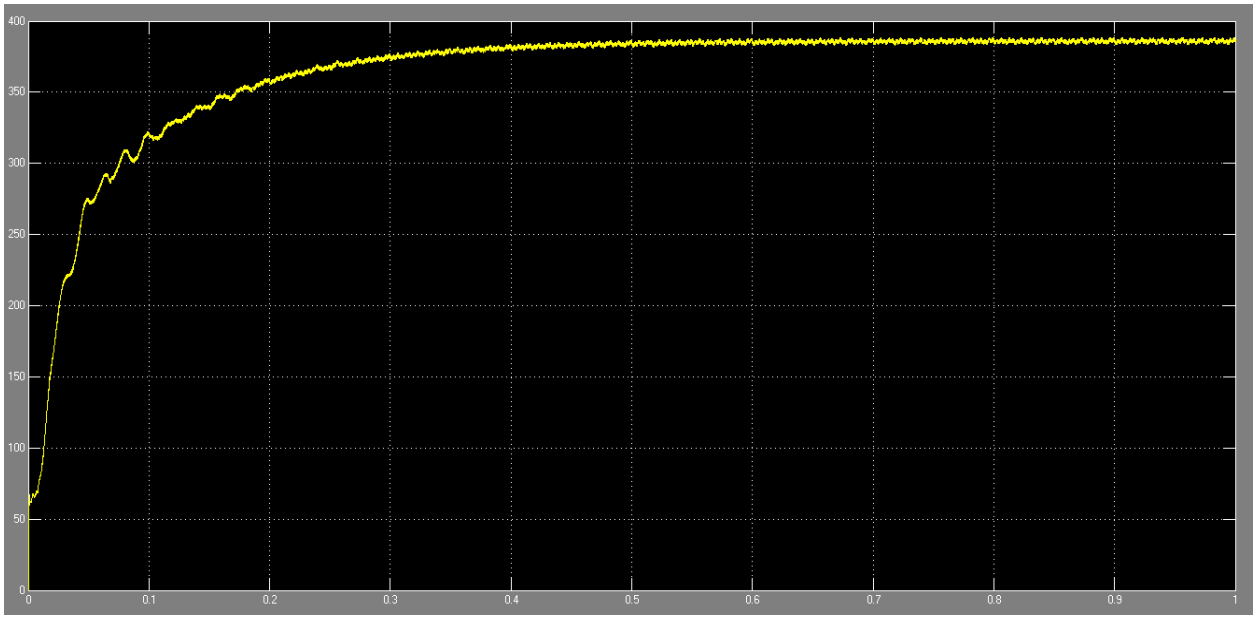

FIGURE 7.2.5 LUO CONVERTER OUTPUT

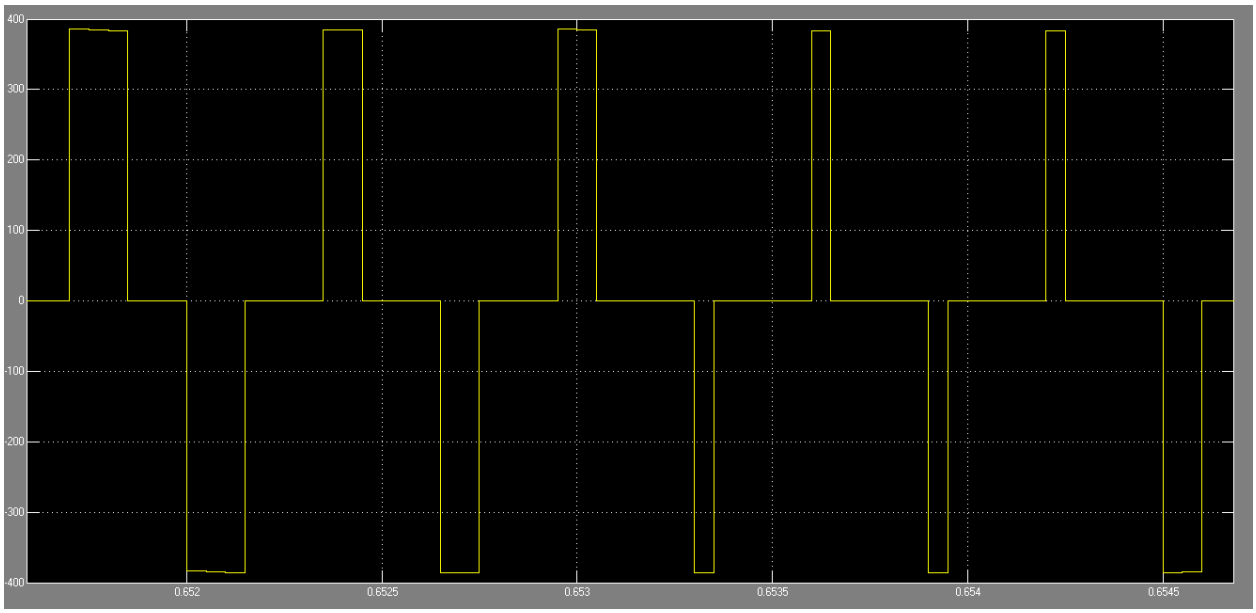

FIGURE 7.2.6 OVERALL VOLTAGE OUTPUT WAVEFORM

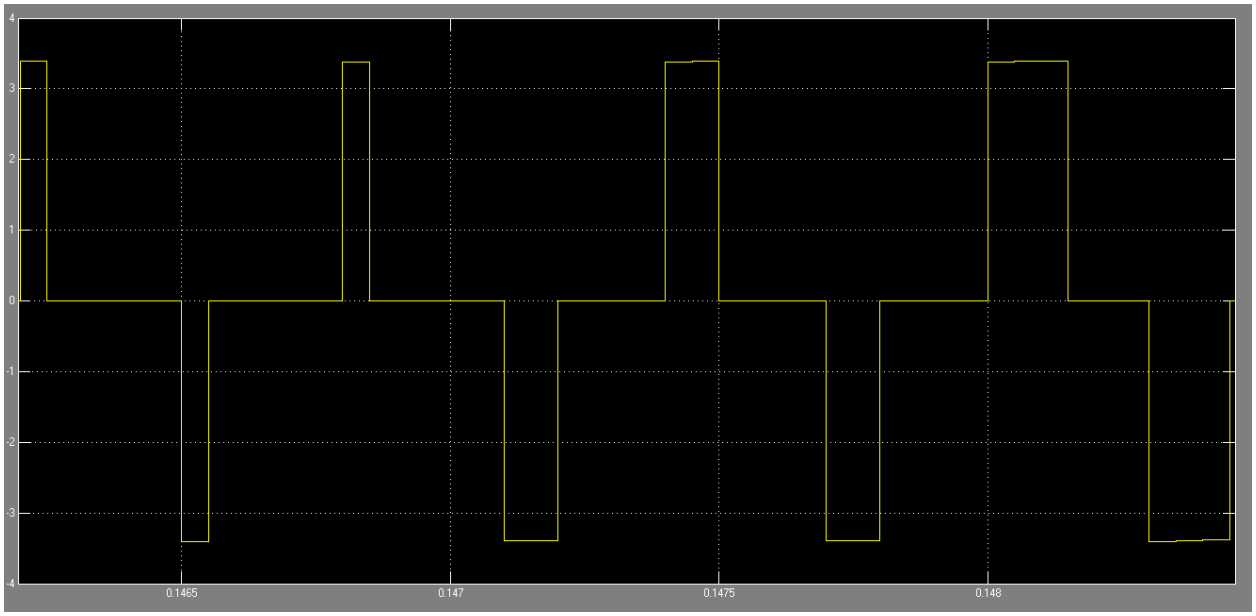

FIGURE 7.2.7 OVERALL CURRENT OUTPUT WAVEFORM

CONCLUSION

A grid-connected hybrid PV–wind-battery-based power evacuation scheme for household application is proposed. The proposed hybrid system provides an elegant integration of PV and wind source to extract maximum energy from the two sources. It is realized by a DC-DC luo converter followed by a conventional singlr phase full-bridge inverter. A versatile control strategy which achieves a better utilization of PV, wind power, battery capacities without effecting life of battery, and power flow management in a grid-connected hybrid PV–wind-battery-based system feeding ac loads is presented. Detailed simulation studies are carried out to ascertain the viability of the scheme. The experimental results obtained are in close agreement with simulations and are supportive in demonstrating the capability of the system to operate either in grid feeding or in stand-alone modes. The proposed configuration is capable of supplying uninterruptible power to ac loads, and ensures the evacuation of surplus PV and wind power into the grid.

REFERENCES

[1] F. Valenciaga and P. F. Puleston, "Supervisor control for a stand-alone hybrid generation system using wind and photovoltaic energy," *IEEE Trans. Energy Convers.*, vol. 20, no. 2, pp. 398–405, Jun. 2005.

[2] C. Liu, K. T. Chau, and X. Zhang, "An efficient wind–photovoltaic hybrid generation system using doubly excited permanent-magnet brushless machine," *IEEE Trans. Ind. Electron.*, vol. 57, no. 3, pp. 831–839, Mar. 2010.

[3] W. Qi, J. Liu, X. Chen, and P. D. Christofides, "Supervisory predictive control of standalone wind/solar energy generation systems," *IEEE Trans. Control Syst. Technol.*, vol. 19, no. 1, pp. 199–207, Jan. 2011.

[4] F. Giraud and Z. M. Salameh, "Steady-state performance of a grid-connected rooftop hybrid wind-photovoltaic power system with battery storage," *IEEE Trans. Energy Convers.*, vol. 16, no. 1, pp. 1–7, Mar. 2001.

[5] S.-K. Kim, J.-H. Jeon, C.-H. Cho, J.-B. Ahn, and S.-H. Kwon, "Dynamic modeling and control of a grid-connected hybrid generation system with versatile power transfer," *IEEE Trans. Ind. Electron.*, vol. 55, no. 4, pp. 1677–1688, Apr. 2008.

[6] M. Dali, J. Belhadj, and X. Roboam, "Hybrid solar–wind system with battery storage operating in grid-connected and standalone mode: Control and energy management—Experimental investigation," *Energy*, vol. 35, no. 6, pp. 2587–2595, Jun. 2010.

[7] W. D. Kellogg, M. H. Nehrir, G. Venkataramanan, and V. Gerez, "Generation unit sizing and cost analysis for stand-alone wind, photovoltaic, and hybrid wind/PV systems," *IEEE Trans. Energy Convers.*, vol. 13, no. 1, pp. 70–75, Mar. 1998.

[8] L. Xu, X. Ruan, C. Mao, B. Zhang, and Y. Luo, "An improved optimal sizing method for wind-solar-battery hybrid power system," *IEEE Trans. Sustain. Energy*, vol. 4, no. 3, pp. 774–785, Jul. 2013.

[9] B. S. Borowy and Z. M. Salameh, “Dynamic response of a standalone wind energy conversion system with battery energy storage to a wind gust,” *IEEE Trans. Energy Convers.*, vol. 12, no. 1, pp. 73–78, Mar. 1997.

[10] S. Bae and A. Kwasinski, “Dynamic modeling and operation strategy for a microgrid with wind and photovoltaic resources,” *IEEE Trans. Smart Grid*, vol. 3, no. 4, pp. 1867–1876, Dec. 2012.

[11] C. W. Chen, C. Y. Liao, K. H. Chen, and Y. M. Chen, “Modeling and controller design of a semi-isolated multi-input converter for a hybrid PV/wind power charger system,” *IEEE Trans. Power Electron.*, vol. 30, no. 9, pp. 4843–4853, Sep. 2015.

[12] M. H. Nehrir, B. J. LaMeres, G. Venkataramanan, V. Gerez, and L. A. Alvarado, “An approach to evaluate the general performance of stand-alone wind/photovoltaic generating systems,” *IEEE Trans. Energy Convers.*, vol. 15, no. 4, pp. 433–439, Dec. 2000.

[13] W. M. Lin, C. M. Hong, and C. H. Chen, “Neural-network-based MPPT control of a stand-alone hybrid power generation system,” *IEEE Trans. Power Electron.*, vol. 26, no. 12, pp. 3571–3581, Dec. 2011.

[14] F. Valenciaga, P. F. Puleston, and P. E. Battaiotto, “Power control of a solar/wind generation system without wind measurement: A passivity/ sliding mode approach,” *IEEE Trans. Energy Convers.*, vol. 18, no. 4, pp. 501–507, Dec. 2003.

[15] T. Hirose and H. Matsuo, “Standalone hybrid wind-solar power generation system applying dump power control without dump load,” *IEEE Trans. Ind. Electron.*, vol. 59, no. 2, pp. 988–997, Feb. 2012.

[16] S. A. Daniel and N. Ammasaigounden, “A novel hybrid isolated generating system based on PV fed inverter-assisted wind-driven induction generators,” *IEEE Trans. Energy Convers.*, vol. 19, no. 2, pp. 416–422, Jun. 2004.

[17] R. G. Wandhare and V. Agarwal, “Novel integration of a PV-wind energy system with enhanced efficiency,” *IEEE Trans. Power Electron.*, vol. 30, no. 7, pp. 3638–3649, Jul. 2015.

[18] Z. Qian, O. Abdel-Rahman, and I. Batarseh, “An integrated four-port DC/DC converter for renewable energy applications,” *IEEE Trans. Power Electron.*, vol. 25, no. 7, pp. 1877–1887, Jul. 2010.

[19] F. Nejabatkhah, S. Danyali, S. H. Hosseini, M. Sabahi, and S. M. Niapour, “Modeling and control of a new three-input DC–DC boost converter for hybrid PV/FC/battery power system,” *IEEE Trans. Power Electron.*, vol. 27, no. 5, pp. 2309–2324, Feb. 2014.